Regulating Charge Injection in Ambipolar Organic Field-Effect Transistors by Mixed Self-Assembled Monolayers

Yong Xu,[†,||] Kang-Jun Baeg,[‡,||] Won-Tae Park,[†] Ara Cho,[†] Eun-Young Choi,[§] and Yong-Young Noh*,[†]

[†]Department of Energy and Materials Engineering, Dongguk University, 26 Pil-dong, 3-Ga, Jung-gu, Seoul 100-715, Republic of Korea

[‡]Nano Carbon Materials Research Group, Korea Electrotechnology Research Institute (KERI), 12 Bulmosan-ro 10 Beon-gil, Seongsan-gu, Changwon, Gyeongsangnam-do 642-120, Republic of Korea

[§]Nuclear Fuel Cycle Development Group, Korea Atomic Energy Research Institute, 1035 Daedok-daero, Yuseong-gu, Daejeon 305-353, Republic of Korea

Ⓢ *Supporting Information*

ABSTRACT: We report on a technique using mixed self-assembled monolayers (SAMs) to finely regulate ambipolar charge injection in polymer organic field-effect transistors. Differing from the other works that employ single SAM specifically for efficient charge injection in *p*-type and *n*-type transistors, we blend two different SAMs of alkyl- and perfluoroalkyl thiols at different ratios and apply them to ambipolar OFETs and inverter. Thanks to the utilization of ambipolar semiconductor and one SAM mixture, the device and circuit fabrications are facile with only one step for semiconductor deposition and another for SAM treatment. This is much simpler with respect to the conventional scheme for the unipolar-device-based complementary circuitry that demands separate deposition and processing for individual *p*-channel and *n*-channel transistors. Our results show that the mixed-SAM treatments not only improve ambipolar charge injection manifesting as higher hole- and electron-mobility and smaller threshold voltage but also gradually tune the device characteristics to reach a desired condition for circuit application. Therefore, this simple but useful approach is promising for ambipolar electronics.

KEYWORDS: *ambipolar, charge injection, conjugated molecules, organic filed-effect transistors, self-assembled monolayer*
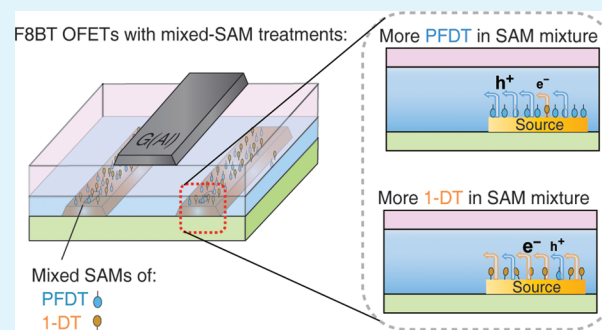
1. INTRODUCTION

Solution processable π-conjugated molecules are promising to compose organic devices for wide applications in large-area, flexible, transparent, environmentally friendly, and low-cost electronics.[1−3] As a core feature of those achievements, unconventional deposition and patterning techniques especially solution-based printing will shift semiconductor manufacturing to a new paradigm by replacing the present costly photo-lithography and vacuum-based processes.[4] Printed organic field-effect transistors (OFETs) that stand for the primary building blocks of numerous expected applications have been intensively studied.[5,6] At the beginning of OFET research, for the sake of simplicity and accessibility most of devices were built on doped Si wafer covered with thermally grown SiO_2 that serve as the gate electrode and gate dielectric, respectively. Such a rigid substrate limited the flexibility of the composed circuits even if devices themselves would be quite soft. Moreover, SiO_2 contains high density of hydroxyl groups known as electron traps significantly suppressing *n*-type device characteristics thereby the majority OFETs so far has been *p*-type transistors.[7] This unipolarity impedes the interesting OFET applications using ambipolar transport characteristics in organic semi-conductors (OSCs). In fact, there are plenty of OSCs having ambipolar properties,[8] in particular, the recently reported donor−acceptor copolymers (e.g., diketopyrrolopyrrole dithienylthieno[3,2-*b*] thiophene (DPP-DTT)) that exhibit small bandgaps and unprecedentedly high carrier mobility up to 10 cm^2/(V s).[9] In order to trigger the intrinsic nature of ambipolar transport in OSC, researchers started to use the siloxane-based polymer dielectrics (e.g., benzocyclobutene (BCB)) or capping layers of alkyl-silane self-assembled monolayers (SAMs),[10] and since then, ambipolar related applications were extensively investigated.[1] For instance, Zaumseil et al. demonstrated light-emitting OFETs based on ambipolar polymeric semiconductors.[11]

Ambipolar OFETs are appealing for complementary metal-oxide-semiconductor (CMOS) organic integrated circuits (ICs) as they can much simplify circuit design and greatly improve circuit performance with respect to the present unipolar device-based CMOS ICs.[12] On the other hand, the conventional Si-

based CMOS technology necessitates individual p-MOS and n-MOS transistors that have to be processed separately by different doping and patterning, that is, lots of steps and photo masks. Such a technology is time-consuming and expensive. If solution-processed ambipolar OFETs were feasible, the fabrication of organic CMOS ICs will be much simpler and the manufacturing cost can be greatly reduced. One can simply make ambipolar OFETs at once by fast printing OSCs over large-area, flexible and transparent substrates and the p- and n-channel operations will self-adapt depending on the applied biases. By optimization of the nanostructure of printed semiconductor films, for example, via multistripes of p- and n-type OSCs[13] or nanostripes of ambipolar OSC,[14] high-performance ambipolar OFETs and logic circuits have been demonstrated. However, a big challenge still remains for ambipolar OFETs: unbalanced p- and n-channel characteristics. Except for the inherent causes of OSC (e.g., different density of states between conduction and valence bands, different electron/hole traps, native doping), charge injection is a critical issue that needs to be solved first. OSCs are often used without doping, namely intrinsic semiconductors, the charge injection is essentially through thermal activation and the injection barrier is thus a key factor determining the resultant device performance.[15] Since almost all OSCs have wide band gap (e.g., >2 eV) and most of the metals that could be used as contact electrode have high work function (WF) (e.g., WF > 4.5 eV), the hole-injection is usually more efficient than the electron-injection. Indeed, this problem can be alleviated by using OSCs with smaller band gaps or applying asymmetric contacts to specifically optimize electron- and hole-injection[16] yet those compromised approaches degrade device performance (e.g., static leakage current and on/off ratio) and increase fabrication complexity (i.e., cost). A better way is to treat the contacts using SAMs or charge injection layers to control the WFs.[17,18] As the hole- and electron-injection barriers share the band gap of OSC and each treatment has its specific function for only one injection, thereby reducing one injection barrier by those treatments will inevitably increase another. Are there any methods that improve both hole- and electron-injection or enable systematic control of the injection mechanism for ambipolar OFETs?

In this paper, we present a simple method to finely control the WF of metal electrodes by using a mixed SAM consisting of alkyl- and perfluoroalkyl thiols. Dipping the samples in two SAM-dispersed solutions with various mixing ratios changes the surface coverage of alkyl- and fluoroalkyl-SAMs and the Au electrodes' WF is constantly modulated from 4.4 to 5.7 eV. The treated Au bottom-contact source/drain electrodes are applied to ambipolar OFETs with poly(9,9-di-n-octylfluorene-alt-benzothiadiazole) (F8BT) to investigate ambipolar charge injection properties. The mixed-SAM treatments greatly improve the performance for both p- and n-channel operations and demonstrate tunability of device characteristics. The application of mixed-SAM treated F8BT OFETs in CMOS inverter confirms the feasibility of regulating ambipolar charge injection for ambipolar electronics.

2. EXPERIMENTS

One-side polished Corning Eagle 2000 glass served as substrate for all devices after cleaning sequentially in ultrasonic bath with deionized water, acetone, and isopropanol for 10 min for each. The Au source/drain electrodes (corresponding channel width/length $W/L = 1$ mm/20 μm) were defined using the conventional lift-off photolithography

and cleaned with O_2 plasma for 200 s. Next, the Au source/drain electrodes were treated by a mixed 1H,1H,2H,2H-perfluorodecane-thiol (PFDT) (Aldrich) and 1-decanethiol (1DT) (Aldrich) solution with immersing the samples into diluted PFDT and 1DT solution in isopropanol (5−10 mM) for 30 min. Afterward, all the samples were rinsed thoroughly by isopropanol to remove the unbound PFDT and 1DT molecules. After that, the organic semiconductor poly(9,9-di-n-octylfluorene-alt-benzothiadiazole) (F8BT, American Dye Source Inc.) was dissolved in anhydrous- p-xylene and chlorobenzene (1 wt %). The solution was heated by placing on a hot plate at 80 °C for complete dilution and then spin-coated onto substrate (2000 rpm, 60 s) in a nitrogen-filled glovebox as soon as possible in order to avoid solidification. The F8BT films were annealed at 150 °C for 20 min to remove residual solvent and improve the molecular order. Poly(methyl methacrylate) (PMMA, Aldrich, M_w = 120 k Da) was used as top-gate dielectric after dissolving in anhydrous n-butyl acetate (80 mg/mL) without purification. The PMMA solution was filtered via 0.2 μm syringe filter and spin-coated at 2000 rpm onto the semiconductor film, yielding a thickness of 400−450 nm. Device fabrication was completed with thermal evaporation of a thin layer of aluminum as the gate electrode via shadow masks.

The electrical characterizations were carried out using a semiconductor parameter analyzer HP 4156C and an impedance analyzer HP 4284A in a nitrogen-filled glovebox. The WF of functionalized Au was measured by a RIKEN AC-2 surface analyzer, which scanned the Au surface using deuterium UV lamp from 3.4 to 6.2 eV. As the UV spot area is 2−4 mm, we measured 2−3 places over a total area of 150 × 150 mm for each sample and counted the rates (cps) at different locations. The work function was calculated as point of contact of X-axis that is energy using linear regression of counting rate values. The wettability of mixed-SAM treated Au surface was measured from static contact angle using a contact angle goniometer (Phoenix-300, Surface Electro Optics) equipped with a digital image acquisition system and an automatic liquid dispenser. The contact angle was determined by numerical fitting algorithm using side view of drops. Elemental composition of mixed-SAM treated Au was analyzed by X-ray photoelectron spectroscopy (PHI 5000 VersaProbe II Scanning XPS Microprobe, ULVAC-PHI Inc.). XPS measurement provided the coverage concentration of SAM-treated Au for each element that was carbon, fluorene, hydrogen, and oxygen.

3. RESULTS AND DISCUSSION

The π-conjugated polymer F8BT was used as the active material for this study, cf. Figure 1a. F8BT possesses electron withdrawing (benzothiadiazole unit) and donating group (fluorine unit) in one polymer chain thereby F8BT has a relatively high electron affinity of 3.3 eV and a high ionization potential of 5.9 eV, making it very suited for the electron-transporting layer in photovoltaic cells and the light-emitting layer in organic light-emitting diodes.[11,19] Still, previous studies of F8BT OFETs have demonstrated well-balanced and reliable ambipolar transport characteristics albeit the relatively low electron and hole mobility ($10^{-3}\sim 10^{-4}$ cm^2/(V s)) with respect to the state-of-the-art high-performance conjugated polymers due to its amorphous nature.[20] Therefore, F8BT is an appropriate material vehicle to probe charge injection mechanism in ambipolar OFETs without significant side effects such as change of OSC crystallinity. Top-gate and bottom-contact (TG/BC) F8BT OFETs were fabricated for this study owing to their several advantages over other device structures. The effective removal of electron traps by using hydroxyl-free top-gate dielectric (PMMA),[7] large injection area through the staggered bottom-contacts,[21] and improved reliability and stability because of the upper-laid dielectric and gate electrode[22] facilitates the ambipolar charge transport in such OFETs. Therefore, the influences of charge injection barrier can be more explicitly identified.
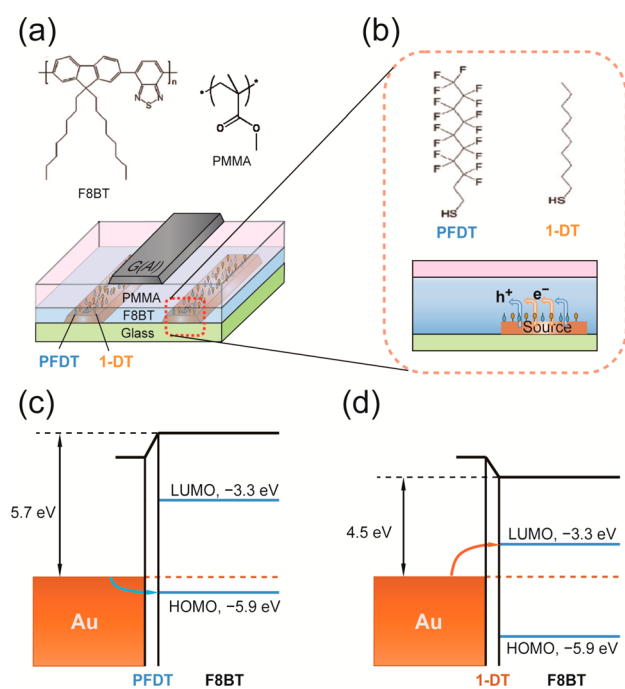
Figure 1. (a) Device structure of the studied top-gate/bottom-contact F8BT OFETs, where the molecular structure of F8BT and PMMA are illustrated. (b) Close look at the charge injection at the source electrode/OSC interface where the SAM interlayers of 1DT and PFDT selectively improving electron- and hole-injection are shown. Energy diagrams of charge injection with using different SAM interlayer (PFDT (c) and 1DT (d)) from Au contacts into F8BT polymer semiconductor, where the second interface dipoles between SAM and F8BT are not included.

Based on the Schottky–Mott model,[23] the energetic barriers to hole- and electron-injection are determined by the difference between the WF of metal source/drain electrodes and the highest occupied molecular orbital (HOMO) and the lowest unoccupied molecular orbital (LUMO) of OSC, respectively, if corrected for interface dipoles. To manipulate the corresponding injection barriers, we utilized two different SAMs of 1DT and PFDT to treat the BC Au electrodes. The alkanethiols and perfluorinated alkanethiols deposited on the Au electrodes form uniform SAMs and induce opposite electrostatic dipole moments, associated with the molecules and the Au–S bond at the interface. This abruptly changes the Au's WF in different directions; that is, 1DT decreases the Au's WF while PFDT increases it, see Figure 1c and d.

Differing from the previous works on OFETs where only one specific SAM was applied,[10,24] in this study, we employed a SAM mixture incorporating 1DT and PFDT for a fine and continuous manipulation of Au's WF. The ratio of mixed SAMs varies according to the different molecular concentrations (1DT:PFDT) in dipping solution as 10:0, 8:2, 5:5, 3:7, 2:8, 1:9, and 0:10. We examined the surface energy of the Au electrodes before and after SAM treatment. Figure 2 shows the contact angles of chlorobenzene solvent on the treated Au surfaces. Chlorobenzene is chosen for its common application to OSC deposition and also for its solvent use in coating F8BT in this study. The Au surfaces after cleanness by oxygen plasma display a relatively high surface energy showing as a contact angle of 54.5°. Interestingly, the mixed-SAM treatments cause very different contact angles, yet with a predictable tendency depending on the mixture ratio. A higher PFDT concentration
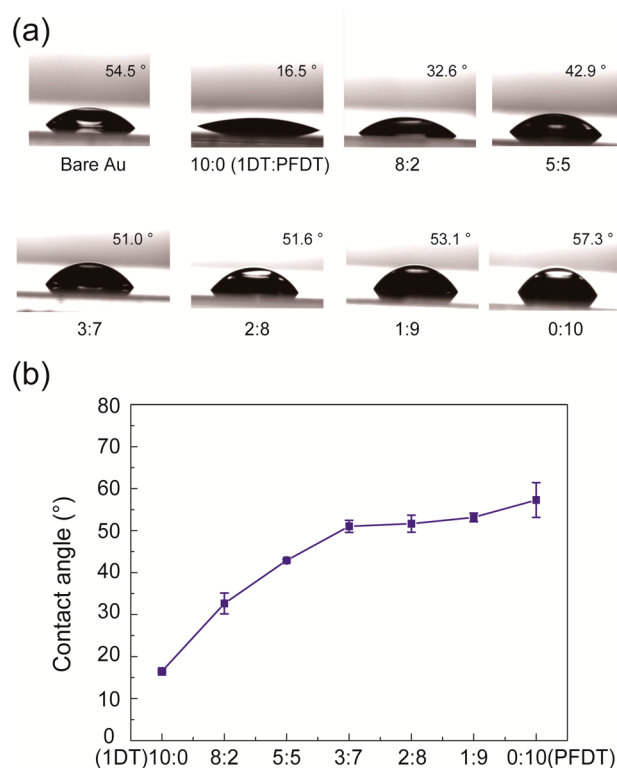

Figure 2. (a) CCD camera images of the static contact angles of chlorobenzene on O$_2$ plasma cleaned Au surface and 1DT:PFDT mixed-SAM treated Au surfaces with various mixing ratios. (b) The correspondingly measured static contact angles.

in the SAM mixture leads to a larger contact angle, up to ∼57.3° for 100% PFDT as compared to the lowest 16.5° for 100% 1DT, see Figure 2b and Table 1. It indicates that the

Table 1. Contact Angle, Surface Coverage and Work Function of Bottom-Contact Au Electrodes with O$_2$ Plasma Cleaning or with Mixed-SAM Treatment at Various 1DT:PFDT Ratios

mixed SAM ratio (1DT:PFDT)	contact angle (deg)	surface coverage (at. %)	work function (eV)
pristine (O$_2$ plasma)	54.5	0	5.0
(1DT) 10:0	16.5	2.3	4.5
8:2	32.6	6.28	4.7
5:5	42.9	16.3	5.0
3:7	51.0	22.7	5.2
2:8	51.6	26.0	5.3
1:9	53.1	35.1	5.5
0:10 (PFDT)	57.3	38.5	5.7

fluorinated alkyl-chains in the PFDT produce more hydrophobic surfaces with smaller surface energy than those treated by 1DT. Note that the lower surface energy may reduce the OSC film thickness on the SAM-treated metal electrodes, probably resulting in a lower contact resistance. This is because in staggered OFETs (e.g., TG/BC) the charge carriers have to traverse "more neutral" OSC bulk to attain the channel,[25] which is an important contributor to the contact resistance. The thinner OSC films on BC Au electrodes will shorten the distance for the vertical carrier traveling so that the contact resistance is decreased in part.[15]
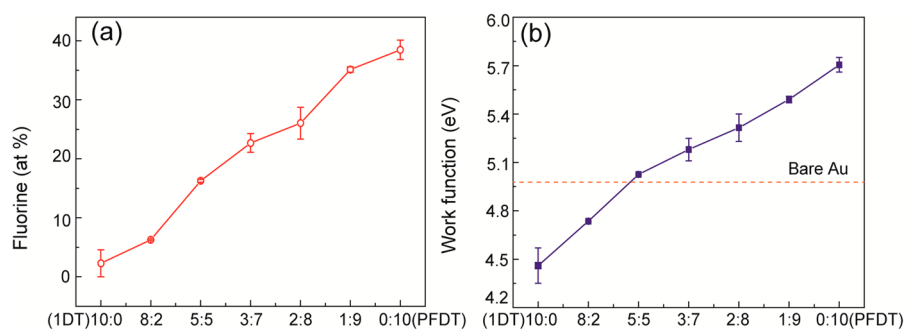
Figure 3. (a) Fluorine surface coverage measured by XPS and (b) corresponding work functions of 1DT:PFDT mixed-SAM treated Au electrodes.
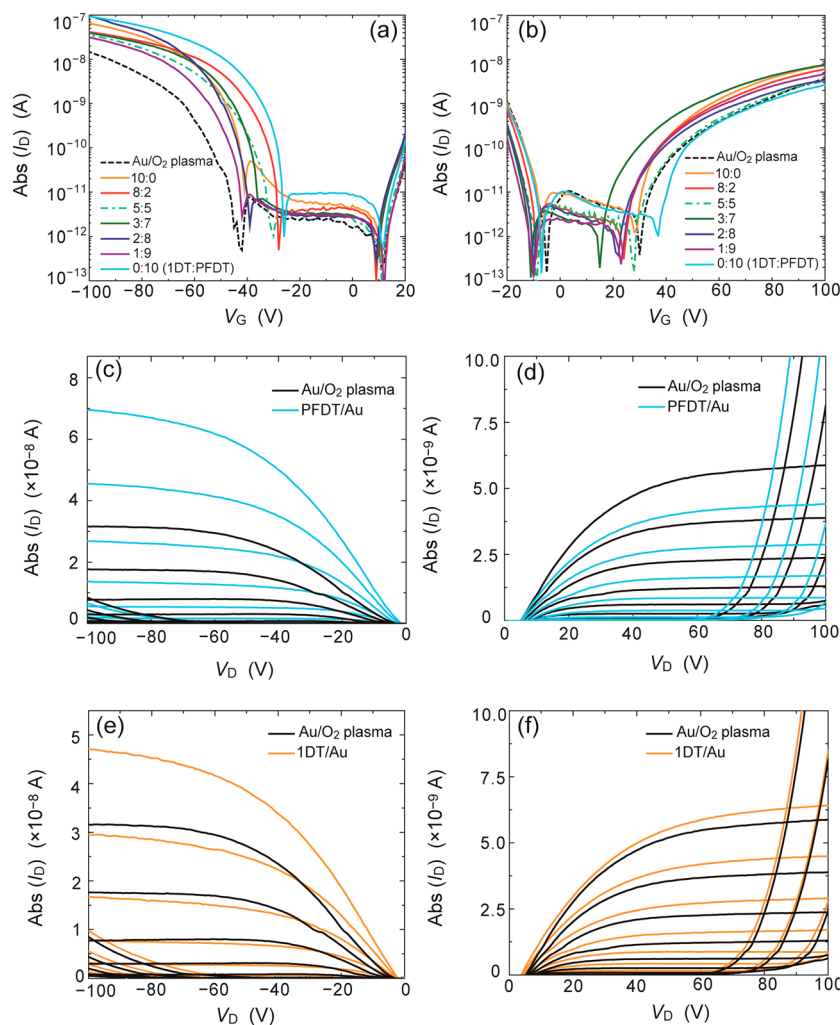

Figure 4. (a and b) Linear transfer characteristic of the ambipolar F8BT OFETs in *p*-channel regime at the drain voltage $V_D = -5$ V and in *n*-channel regime at $V_D = 5$ V with various mixed-SAM treatments, respectively. (c and d) *p*-channel and *n*-channel output characteristics of the F8BT OFETs with only bare Au electrodes and Au electrodes treated by PFDT, respectively. (e−f) Identical to parts c and d except for the different SAM of 1DT.

The surface coverage of fluorine atom and the Au's WF after mixed-SAM treatments were measured by X-ray photoelectron spectroscopy (XPS) and ultraviolet photoemission spectroscopy (UPS), respectively. The XPS data show that the surface coverage of fluorine atom increases from ∼0 to ∼40% as the 1DT:PFDT ratio changing from 10:0 to 0:10; see Figure 3a. More importantly, the UPS measurements turn out that the Au electrodes' WF is changed gradually from 4.4 to 5.7 eV with the 1DT:PFDT ratio varying from 10:0, 8:2, 5:5, 3:7, 2:8, 1:9, to 0:10, cf. Figure 3b. With respect to the reference WF of 5.0 eV

for bare Au, a decrease in the Au's WF is obtained with incorporating predominantly 1DT yet PFDT-rich mixtures lead to higher WF up to 5.7 eV. They all are in good agreement with the literature.[20] Such a finely and systematically regulated WF of the contact electrodes can be expected to modulate the charge injection for desired unipolar and ambipolar charge transports. In fact, similar approaches using diverse SAM combinations have been applied to organic light-emitting diodes (OLEDs)[26] where the charge injection barriers are critical determinants and optimization of injection barrier

immediately translated into performance improvements, for example, greater light emitting efficiency and brightness.[27] For OFETs, however, the related reports are rare,[28] as the charge injection and subsequent charge transport are much more complex than in OLEDs and the energetic barrier is only one of the factors affecting charge injection. For the promising ambipolar OFETs, efficient injections of both hole and electron are of great research interest.

Therefore, we apply this WF regulation technique via mixed-SAM treatment to investigate the influences on the p-channel or n-channel properties in ambipolar F8BT OFETs. Parts a and b of Figure 4 illustrate the linear transfer characteristics with various 1DT:PFDT ratios in SAM mixture, where the data of using pristine (O₂ plasma cleaned) Au electrodes are also included for comparison. One can readily see ambipolar characteristics, and the reference OFETs exhibit hole- and electron-mobility of 3.22×10^{-4} cm²V⁻¹s⁻¹ and 7.79×10^{-5} cm²V⁻¹s⁻¹, respectively, which was evaluated by the Y function method.[29] Also, the different SAM treatments shift the transfer curves laterally and vertically regarding the reference OFETs. The lateral shifts correspond to changes of threshold voltage (V_T) and the vertical shifts signify mobility variations. As discussed above, PFDT provides a lowered barrier to hole-injection, and hence, the PFDT-dominated ratios indeed reduce V_{Th} (= −45.9 V) for p-channel operation and greatly increase hole mobility ($\mu_h = 3.05 \times 10^{-3}$ cm² V⁻¹ s⁻¹) versus the reference ($V_{Th} = -59.2$ V, $\mu_h = 3.22 \times 10^{-4}$ cm² V⁻¹ s⁻¹). It has been reported that large injection barrier not only limits the overall charge transport manifesting as small apparent mobility and high contact resistance but also raises V_T due to the futile potential drop at contacts.[30,31] To verify the contact improvements, we measured the output characteristics, cf. Figure 4c. One can find superlinearity at small drain voltages for the reference OFETs, indicative of non-Ohmic contacts due to the large hole-injection barrier. After PFDT-SAM treatment, the current suppression is alleviated with good linearity in linear region so that output current is much enhanced. Figure 4d shows the output characteristics of n-channel operation where the PFDT-SAM treatment appears to be detrimental to the electron-injection, as expected.

When the 1DT-dominated ratios are used, the hole-injection barrier should be elevated and theoretically p-channel characteristics will be degraded. Yet, the 100% 1DT corresponding to a large hole-injection barrier of 1.4 eV (cf. Figure 1d) demonstrates also improved performance of p-channel operation ($V_{Th} = -55.3$ V, $\mu_h = 2.34 \times 10^{-3}$ cm² V⁻¹ s⁻¹) as compared to the reference, see Figure 4e. More extracted parameters are summarized in Table 2. Cheng et al. observed the similar result and interpreted it in terms of the smaller OSC film thickness on top of 1DT-treated Au surface due to the slightly lower surface energy induced by 1DT treatment than O₂ plasma treatment.[20] Note that in their work xylene was used to deposit OSC and to testify surface energy and the obtained contact angels were 5.0°, 15.5°, and 76.3° for O₂ plasma, 1DT and PFDT treatments, respectively. The higher contact angels after SAM-treatments imply that the OSC film deposited atop of the SAM-treated electrode surface would be thinner, as discussed above by Cheng et al.[20] However, we employed chlorobenzene in this study and observed contact angels of 54.5°, 16.5°, and 57.3° for O₂ plasma, 1DT, and PFDT treatments, respectively. The surface energy was double checked by using deionized water, see Figure S1 in Supporting Information. Based on these experimental results, 1DT here

Table 2. Fundamental Parameters of the F8BT OFETs (W = 1 mm, L = 20 μm), where the Mobility and Threshold Voltage Were Extracted by the Y Function Method

mixed SAM ratio (1DT:PFDT)	P-channel operation		N-channel operation	
	mobility (cm²/(V s))	threshold voltage (V)	mobility (cm²/(V s))	threshold voltage (V)
pristine (O₂ plasma)	3.22×10^{-4}	−59.2	7.79×10^{-5}	52.3
(1DT) 10:0	2.34×10^{-3}	−55.3	2.42×10^{-4}	51.4
8:2	1.18×10^{-3}	−42.7	1.83×10^{-4}	50.9
5:5	1.14×10^{-3}	−52.4	9.07×10^{-5}	52.1
3:7	1.22×10^{-3}	−47.7	2.24×10^{-4}	46.5
2:8	2.11×10^{-3}	−53.4	1.32×10^{-4}	51.3
1:9	1.12×10^{-3}	−57.2	1.46×10^{-4}	50.6
0:10(PFDT)	3.05×10^{-3}	−45.9	7.11×10^{-5}	52.4

corresponding to smaller contact angle against pristine Au would not reduce the F8BT film thickness on the 1DT-treated Au surfaces and thus there should be other significant mechanisms responsible for the improved hole-injection. Since charge carriers have to be first injected from Au electrodes through the ultrathin SAM interlayer to reach the OSC by tunneling, a smaller tunneling barrier is vital to the interface injection especially for those over large energy barriers. It is interesting to note that relative to PFDT, 1DT forms a thinner and more disordered and loosely packed monolayer that notably improves the hole-injection capability in spite of the large energy barrier predicted by the Schottky−Mott rule. Analogous behaviors have been reported for the contact interlayers of metal oxides such as Al₂O₃ and MoO₃. When the interlayer is resistive (e.g., Al₂O₃), a ultrathin film is dispensable to enable effective charge tunneling and transfer.[32] Moreover, the interface disorders or defects (i.e., generation and combination centers) have been evidenced to be very utile in producing Ohmic contacts without strict requirement of small Schottky barrier,[33,31] even for silicon MOSFETs.[23] For a complete overview of injection-related improvements, we compared the output characteristics of 1DT-treated OFETs with the reference and found that the nonlinearity and output current are all ameliorated; see Figure 4e and f. Hence, 1DT is favorable not only to electron-injection but also to hole-injection.

As 1DT is mixed with a small amount of PFDT, the hole-injection appears to be degraded perhaps due to the compensation of PFDT that significantly alters the surface properties of 1DT. However, the purpose of using 1DT is to reduce the electron-injection barrier for better n-channel performance. From Table 2, all SAM mixtures including any proportion of 1DT indeed give rise to higher electron-mobility and smaller V_{Te}, for example, $\mu_e = 1.46 \times 10^{-4}$ cm² V⁻¹ s⁻¹ and $V_{Te} = 50.6$ V for 10% 1DT versus reference $\mu_e = 7.79 \times 10^{-5}$ cm² V⁻¹ s⁻¹ and $V_{Te} = 52.3$ V. One may notice that the optimal situation does not arise from pure 1DT treatment but around 30% 1DT, at which μ_e is comparable to the highest value at 100% 1DT yet V_T is smaller than that for pure 1DT. Therefore, the mixed-SAM treatment can be adopted to finely tune the device characteristics. This is the main difference between single-SAM and mixed-SAM treatments. It is known that for practical applications such as CMOS ICs many parameters should be considered concurrently for high performance and the matched p-channel and n-channel characteristics. High and balanced hole- and electron-mobility, small and comparable
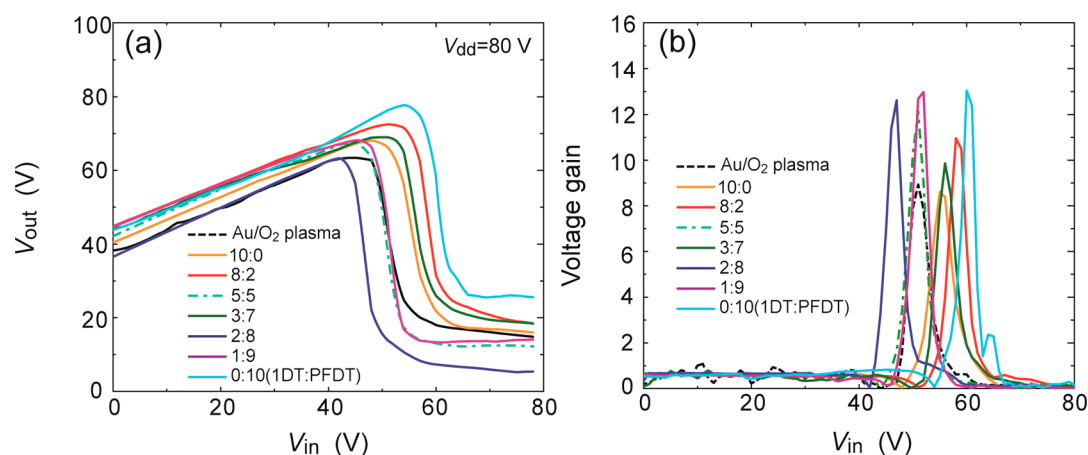
Figure 5. (a) Voltage transfer characteristics of complementary ambipolar F8BT OFETs-based inverters with various mixed-SAM treatments where (the device dimensions are W_p/L_p = 1 mm/20 μm and W_n/L_n = 5 mm/20 μm). (b) The corresponding voltage gains.

threshold voltage (negative V_{Th} and positive V_{Te}) are needed for great gain (fast switching) and large noise margins for both low and high inputs. Small subthreshold swing and V_T and consequently small power supply voltage as well as small "OFF" current are important to reduce power consumption. In a word, this fine regulation of device characteristics via mixed-SAM treatment is promising for ambipolar organic electronics.

To demonstrate the capability of modulating charge injection for better performance in CMOS circuitry, we applied the mixed-SAM treatments to CMOS inverter. Note that the inverter fabrication based on ambipolar F8BT OFETs with mixed-SAM is very simple: only one step for OSC deposition and another step for SAM treatment. The conventional routines of separate p-type and n-type OSC depositions and the corresponding single-SAM treatments are unnecessary, as described in the Introduction. Parts a and b in Figure 5 show the voltage transfer curves (VTCs) and the voltage gain of the CMOS inverters with various mixed-SAM treatments. Interestingly, the results of 5:5 of 1DT:PFDT ratio and pristine Au are close, similarly to their equivalent work functions. Nevertheless, a higher voltage gain (=12) for 5:5-SAM treatment against that using pristine Au (=9) can be still recognized, indicating better performance. Also, the different mixing ratios shift the VTCs, in particular 2:8 ratio leads to both high grain (=12.6) and a pull-down switching around $0.5V_{dd}$ (=40 V). Therefore, the simple process, the tunable device characteristics, and enhanced performance combine to demonstrate the significance of mixed-SAM treatment to ambipolar electronics. Albeit the current results do not show clear tendency with SAM mixture ratio and the tunability and performance improvements are still limited. However, more noticeable progresses could be expected with using high-performance ambipolar semiconductors, for example, donor–acceptor copolymers, two-dimensional atomic films such as graphene and MoS_2 and even carbon nanotubes, with which the composed FETs suffer from Schottky contacts. Thus, the presented mixed-SAM technique could pave the way for high-efficiency ambipolar charge transport.

4. CONCLUSION

In conclusion, we present a straightforward method to finely regulate the ambipolar charge injection in polymer OFETs by means of solution based mixed-SAM treatment instead of the conventional scheme with specific SAMs for p-type and n-type

transistors. The SAM mixture incorporating 1DT and PFDT with different ratios forms a continuous layer atop of the bottom-contact Au electrodes, leading to a gradually modulated work function spanning from 4.4 to 5.6 eV. In agreement with the Schottky–Mott rule, the increased Au's work function by using predominately PFDT reduces the hole-injection barrier and the performance of p-channel operation in F8BT OFETs is greatly improved, with nearly 10 times higher hole-mobility and 15 V smaller threshold voltages. Remarkably, 1DT also improves hole-mobility by a factor of 8 owing to its disordered and loosely packed nature that facilitates interface hole-injection regardless of the theoretically predicted high-energy barrier. This result indicates that interface disorders are vital to ambipolar charge injection and the Schottky–Mott rule may deviate a lot with disordered and/or contaminated interfaces. When the well-packed PFDT SAM is coated for n-channel operation, the electron-mobility is degraded. Yet any portions of 1DT give enhanced n-channel performance and the optimal condition emerges from a mixture of 3:7 (1DT:PFDT) rather than a pure 1DT, highlighting the importance of mixed SAM to ambipolar OFETs. Application of the treated OFETs in CMOS inverter turn out that mixed-SAM can not only improve the voltage gain but also tune the switching transition to approach the half of supply voltage for the maximum noise margins. Therefore, this simple but powerful technique can be very useful in ambipolar electronics for extensive applications.

■ ASSOCIATED CONTENT

Ⓢ Supporting Information

CCD camera images of the static contact angles of deionized (DI) water on O_2 plasma cleaned Au surface and 1DT:PFDT mixed-SAM treated Au surfaces with various mixing ratios and the correspondingly measured static contact angles. This material is available free of charge via the Internet at http://pubs.acs.org/.

■ AUTHOR INFORMATION

Corresponding Author

*Email: yynoh@dongguk.edu.

Author Contributions

∥Y.X. and K.-J.B. contributed equally to this work.

Notes

The authors declare no competing financial interest.

■ REFERENCES

(1) Baeg, K. J.; Caironi, M.; Noh, Y. Y. Toward Printed Integrated Circuits Based on Unipolar or Ambipolar Polymer Semiconductors. *Adv. Mater.* **2013**, *25*, 4210−44.

(2) Minari, T.; Kanehara, Y.; Liu, C.; Sakamoto, K.; Yasuda, T.; Yaguchi, A.; Tsukada, S.; Kashizaki, K.; Kanehara, M. Room-Temperature Printing of Organic Thin-Film Transistors with Π-Junction Gold Nanoparticles. *Adv. Funct. Mater.* **2014**, DOI: 10.1002/adfm.201400169.

(3) Gelinck, G.; Heremans, P.; Nomoto, K.; Anthopoulos, T. D. Organic Transistors in Optical Displays and Microelectronic Applications. *Adv. Mater.* **2010**, *22*, 3778−3798.

(4) Kang, B.; Lee, W. H.; Cho, K. Recent Advances in Organic Transistor Printing Processes. *ACS Appl. Mater. Interfaces* **2013**, *5*, 2302−2315.

(5) Sirringhaus, H. Device Physics of Solution-Processed Organic Field-Effect Transistors. *Adv. Mater.* **2005**, *17*, 2411−2425.

(6) Sirringhaus, H. 25th Anniversary Article: Organic Field-Effect Transistors: The Path Beyond Amorphous Silicon. *Adv. Mater.* **2014**, *26*, 1319−1335.

(7) Baeg, K. J.; Facchetti, A.; Noh, Y. Y. Effects of Gate Dielectrics and Their Solvents on Characteristics of Solution-Processed N-Channel Polymer Field-Effect Transistors. *J. Mater. Chem. C* **2012**, *22*, 21138−21143.

(8) Bisri, S. Z.; Piliego, C.; Gao, J.; Loi, M. A. Outlook and Emerging Semiconducting Materials for Ambipolar Transistors. *Adv. Mater.* **2014**, *26*, 1176−1199.

(9) Li, J.; Zhao, Y.; Tan, H. S.; Guo, Y. L.; Di, C. A.; Yu, G.; Liu, Y. Q.; Lin, M.; Lim, S. H.; Zhou, Y. H.; Su, H. B.; Ong, B. S. A Stable Solution-Processed Polymer Semiconductor with Record High-Mobility for Printed Transistors. *Sci. Rep.* **2012**, *2*, 754.

(10) Noh, Y. Y.; Zhao, N.; Caironi, M.; Sirringhaus, H. Downscaling of Self-Aligned, All-Printed Polymer Thin-Film Transistors. *Nat. Nanotechnol.* **2007**, *2*, 784−789.

(11) Zaumseil, J.; Donley, C. L.; Kim, J. S.; Friend, R. H.; Sirringhaus, H. Efficient Top-Gate, Ambipolar, Light-Emitting Field-Effect Transistors Based on a Green-Light-Emitting Polyfluorene. *Adv. Mater.* **2006**, *18*, 2708−2712.

(12) Lin, Y. F.; Xu, Y.; Wang, S. T.; Li, S. L.; Yamamoto, M.; Aparecido-Ferreira, A.; Li, W.; Sun, H.; Nakaharai, S.; Jian, W. B.; Ueno, K.; Tsukagoshi, K. Ambipolar MoTe$_2$ Transistors and Their Applications in Logic Circuits. *Adv. Mater.* **2014**, *26*, 3263−9.

(13) Cavallini, M.; D'Angelo, P.; Criado, V. V.; Gentili, D.; Shehu, A.; Leonardi, F.; Milita, S.; Liscio, F.; Biscarini, F. Ambipolar Multistripe Organic Field-Effect Transistors. *Adv. Mater.* **2011**, *23*, 5091−5097.

(14) Gentili, D.; Sonar, P.; Liscio, F.; Cramer, T.; Ferlauto, L.; Leonardi, F.; Milita, S.; Dodabalapur, A.; Cavallini, M. Logic-Gate Devices Based on Printed Polymer Semiconducting Nanostripes. *Nano Lett.* **2013**, *13*, 3643−3647.

(15) Natali, D.; Caironi, M. Charge Injection in Solution-Processed Organic Field-Effect Transistors: Physics, Models, and Characterization Methods. *Adv. Mater.* **2012**, *24*, 1357−1387.

(16) Rha, S. H.; Kim, U. K.; Jung, J.; Kim, H. K.; Jung, Y. S.; Hwang, E. S.; Chung, Y. J.; Lee, M.; Choi, J. H.; Hwang, C. S. The Electrical Properties of Asymmetric Schottky Contact Thin-Film Transistors with Amorphous-In$_2$Ga$_2$ZnO$_7$. *IEEE Trans. Electron Devices* **2013**, *60*, 1128−1135.

(17) Zhou, Y. H.; Fuentes-Hernandez, C.; Shim, J.; Meyer, J.; Giordano, A. J.; Li, H.; Winget, P.; Papadopoulos, T.; Cheun, H.; Kim, J.; Fenoll, M.; Dindar, A.; Haske, W.; Najafabadi, E.; Khan, T. M.; Sojoudi, H.; Barlow, S.; Graham, S.; Bredas, J. L.; Marder, S. R.; Kahn, A.; Kippelen, B. A Universal Method to Produce Low-Work Function Electrodes for Organic Electronics. *Science* **2012**, *336*, 327−332.

(18) Baeg, K. J.; Bae, G. T.; Noh, Y. Y. Efficient Charge Injection in P-Type Polymer Field-Effect Transistors with Low-Cost Molybdenum Electrodes through V2O5 Interlayer. *ACS Appl. Mater. Interfaces* **2013**, *5*, 5804−5810.

(19) Gwinner, M. C.; Vaynzof, Y.; Banger, K. K.; Ho, P. K. H.; Friend, R. H.; Sirringhaus, H. Solution-Processed Zinc Oxide as High-Performance Air-Stable Electron Injector in Organic Ambipolar Light-Emitting Field-Effect Transistors. *Adv. Funct. Mater.* **2010**, *20*, 3457−3465.

(20) Cheng, X. Y.; Noh, Y. Y.; Wang, J. P.; Tello, M.; Frisch, J.; Blum, R. P.; Vollmer, A.; Rabe, J. P.; Koch, N.; Sirringhaus, H. Controlling Electron and Hole Charge Injection in Ambipolar Organic Field-Effect Transistors by Self-Assembled Monolayers. *Adv. Funct. Mater.* **2009**, *19*, 2407−2415.

(21) Richards, T. J.; Sirringhaus, H. Analysis of the Contact Resistance in Staggered, Top-Gate Organic Field-Effect Transistors. *J. Appl. Phys.* **2007**, *102*, 094510.

(22) Khim, D.; Lee, W. H.; Baeg, K. J.; Kim, D. Y.; Kang, I. N.; Noh, Y. Y. Highly Stable Printed Polymer Field-Effect Transistors and Inverters via Polyselenophene Conjugated Polymers. *J. Mater. Chem. C* **2012**, *22*, 12774−12783.

(23) Li, S. S. *Semiconductor Physical Electronics*. Second ed.; Springer: Berlin, 2006.

(24) Asadi, K.; Wu, Y.; Gholamrezaie, F.; Rudolf, P.; Blom, P. W. M. Single-Layer Pentacene Field-Effect Transistors Using Electrodes Modified with Self-Assembled Monolayers. *Adv. Mater.* **2009**, *21*, 4109−4114.

(25) Xu, Y.; Liu, C.; Scheideler, W.; Darmawan, P.; Li, S. L.; Balestra, F.; Ghibaudo, G.; Tsukagoshi, K. How Small the Contacts Could Be Optimal for Nanoscale Organic Transistors? *Org. Electron.* **2013**, *14*, 1797−1804.

(26) Wu, K. Y.; Yu, S. Y.; Tao, Y. T. Continuous Modulation of Electrode Work Function with Mixed Self-Assembled Monolayers and Its Effect in Charge Injection. *Langmuir* **2009**, *25*, 6232−6238.

(27) Chen, C. Y.; Wu, K. Y.; Chao, Y. C.; Zan, H. W.; Meng, H. F.; Tao, Y. T. Concomitant Tuning of Metal Work Function and Wetting Property with Mixed Self-Assembled Monolayers. *Org. Electron.* **2011**, *12*, 148−153.

(28) Kim, J.; Rim, Y. S.; Liu, Y.; Serino, A. C.; Thomas, J. C.; Chen, H.; Yang, Y.; Weiss, P. S. Interface Control in Organic Electronics Using Mixed Monolayers of Carboranethiol Isomers. *Nano Lett.* **2014**, *14*, 2946−2951.

(29) Xu, Y.; Minari, T.; Tsukagoshi, K.; Chroboczek, J. A.; Ghibaudo, G. Direct Evaluation of Low-Field Mobility and Access Resistance in Pentacene Field-Effect Transistors. *J. Appl. Phys.* **2010**, *107*, 114507.

(30) Tessler, N.; Roichman, Y. Two-Dimensional Simulation of Polymer Field-Effect Transistor. *Appl. Phys. Lett.* **2001**, *79*, 2987−2989.

(31) Xu, Y.; Liu, C.; Sun, H.; Balestra, F.; Ghibaudo, G.; Scheideler, W.; Noh, Y.-Y. Metal Evaporation Dependent Charge Injection in Organic Transistors. *Org. Electron.* **2014**, *15*, 1738−1744.

(32) Darmawan, P.; Minari, T.; Kumatani, A.; Li, Y.; Liu, C.; Tsukagoshi, K. Reduction of Charge Injection Barrier by 1-nm Contact Oxide Interlayer in Organic Field Effect Transistors. *Appl. Phys. Lett.* **2012**, *100*, 013303.

(33) Hirose, Y.; Kahn, A.; Aristov, V. V.; Soukiassian, P.; Bulovic, V. V.; Forrest, S. R. Chemistry and Electronic Properties of Metal−Organic Semiconductor Interfaces: Al, Ti, in, Sn, Ag, and Au on Ptcda. *Phys. Rev. B: Condensed Matter* **1996**, *54*, 13748−13758.

14499

dx.doi.org/10.1021/am5037862 | *ACS Appl. Mater. Interfaces* 2014, 6, 14493−14499